PHYSICAL REVIEW A VOLUME 25, NUMBER 2 FEBRUARY 1982

High-resolution Rayleigh-Brillouin spectroscopy in the critical mixture nitroethane-isooctane

Y. Garrabos,* G. Zalczer, and D. Beysens

Commissariat à l'Energie Atomique, Division de la Physique, Service de Physique du Solide et de Résonance Magnétique, Boite Postale No. 2, 91190 Gif sur Yvette, France

(Received 12 March 1981)

We report new measurements of the Rayleigh-Brillouin spectrum of a critical binary mixture and review the existing data in this field. We used a double-pass Fabry-Pérot interferometer and a weakly scattering system (nitroethane-isooctane) so that the Brillouin lines were not affected by the wings of the Rayleigh line, even in the immediate vicinity of the critical point. No anomaly was detected in the shift or width or intensity of the Brillouin lines. From the ratio of the intensities of the Rayleigh and Brillouin lines we deduced the ratio of specific heats γ_0, the correlation length ξ_0, and the susceptibility amplitude $(\partial c/\partial\mu)^0_{pT}$, without any hypothesis about light-scattering amplitudes. These values lead to an amplitude ratio $R_\xi^+ R_c^{-1/3}$ in full agreement with the theoretical values.

I. INTRODUCTION

The study of the dispersion and attenuation of sound in critical systems has stimulated theoretical[1-5] and experimental[6-16] interest. The order parameter is not directly observable in this case, but it affects the behavior of other physical quantities through couplings. In most experiments the dispersion and attenuation of sound have been studied with induced ultrasound. The anomalous absorption observed in many systems has been well explained by mode-coupling theories and dynamical scaling[1,5] in the frequency range achievable ($\lesssim$50 MHz). These ultrasonic techniques are accurate but subject to some spurious phenomena: Large volumes are needed whose temperature control is difficult and the ultrasonic pulses can perturb the medium. Light scattering is not affected by these difficulties but other problems arise, mainly the strong increase of the Rayleigh scattering near the critical point (critical opalescence), which can overwhelm the Brillouin lines. Thus, special care must be taken such as using a multipass Fabry-Pérot (FP) interferometer in order to achieve a very high contrast, or using a weakly opalescent system. Finally, the frequency range which the FP experiment investigates is much higher than for ultrasonic experiments, typically about 5 GHz.

The purpose of this paper is to report new experimental results obtained using both a weakly opalescent system (nitroethane-isooctane) and a double pass FP spectrometer, and to review the status of the experimental situation.

Until now three systems have been investigated by both ultrasonic and Brillouin techniques. Ultrasonic measurements have always shown weak negative anomalies in the sound velocity and strong positive anomalies in the sound damping, whereas Brillouin spectroscopy has detected either a corresponding—but much bigger—anomaly in the sound velocity (nitrobenzene + n-hexane,[9-11] nitroethane + isooctane[15,16]), or no anomaly at all (nitrobenzene + n-hexane,[13] nitroethane + 3-methylpentane[12]), or an anomaly in the other direction (triethylamine + water).[7] An anomaly in the sound attenuation has also been reported (nitrobenzene + n-hexane,[11,13] nitroethane + isooctane[16]). However, all the light-scattering experiments which claimed the observation of some anomalies in the sound velocity or the sound damping suffer from the same criticism, namely, using a low-contrast spectrometer which makes it impossible to obtain reliable results near the critical temperature T_c. This limitation still applies to such a weakly opalescent system as nitroethane + isooctane: We will see that the remaining Rayleigh scattering near T_c is spectrally 20 times more intense than the Brillouin lines, which can lead to erroneous conclusions.

II. THEORETICAL BACKGROUND

The spectrum of the light scattered at a transfer wave vector $\vec{q}$ by a liquid mixture consists of three contributions from the three independently decaying thermodynamic parameters: concentration c, entropy s, and pressure p.[17] Each has the structure

$$S_i(q,\omega) = A\left(\frac{\partial(n^2)}{\partial i}\right)^2 k_B T \chi_i G_i(q)\, s_i^0(q,\omega)\,,$$

where A includes the geometrical and electromagnetic factors and is the same for all variables c, s, p; $(\partial(n^2)/\partial i)^2$ expresses the coupling between the light and the fluctuation of the parameter i (the other two are kept constant). The exact structure of this factor is still open to controversy. Indeed, though we can calculate the change in local polarizability, none of the proposed formulas has been universally admitted.[18] However, since the controversial part does not refer to any thermodynamic variable, it is the same for all the con-

tributions. Therefore, the ratios of these contributions are independent of the choice of the formula and we can use any one for their interpretation. χ_i is the susceptibility associated with the parameter i (the other two kept constant) and k_B is the Boltzmann constant so that $k_B T\chi_i$ is the amplitude of the thermal fluctuation of the parameter i. These first three terms express the integrated scattered light at zero wave vector. $G_i(q)$ describes the angular dependence of the integrated intensity, and $s_i^0(q,\omega)$ is a normalized function describing how this light is distributed in the frequency space.

Since the concentration is the order parameter, the associated susceptibility diverges near the critical point as

$$\left(\frac{\partial c}{\partial \mu}\right)_{p,T} = \left(\frac{\partial c}{\partial \mu}\right)^0_{p,T} t^{-\gamma},$$

where t is the reduced temperature difference $(T - T_c)/T_c$ and γ the universal critical exponent $\simeq 1.24$. Moreover, the correlation length ξ of the concentration fluctuations also diverges as

$$\xi = \xi_0 t^{-\nu},$$

where $\nu \simeq 0.63$. Near the critical point this length is no longer negligible compared to λ so the function $G_c(q)$ significantly departs from unity for typically $T - T_c \lesssim 0.3$ K at a scattering angle of 90°.

The time behavior of the concentration fluctuations is also anomalous but since the characteristic frequency (0.5 to 50 kHz) is much smaller than the resolution of our present experiment (100 MHz), we can consider here the line $S_1 = S_c(q,\omega)$ as a δ function of the frequency.

The line $S_2 = S_s(q,\omega)$ associated with entropy fluctuations is isotropic and low frequency (5 MHz). Its intensity is given by

$$I_2 = A\frac{k_B T^2}{C_p}\left(\frac{d(n^2)}{dT}\right)^2_{c,p} = A\frac{C_p - C_v}{C_v}\frac{k_B T}{\beta_s}\left(\frac{\partial (n^2)}{\partial p}\right)^2_{c,s},$$

where β_s is the adiabatic compressibility.

The third contribution $S_3 = S_p(q,\omega)$ is due to pressure fluctuations (Brillouin lines). Its spectrum consists of two symmetrical lines with respect to the incident frequency. The displacement $\pm vq$ is related to the sound velocity v in the mixture. The order of magnitude at a scattering angle of 90° is 4 GHz (2.5×10^{10} rad sec^{-1}):

$$2S_3(q,\omega) = A\frac{k_B T}{\beta_s}\left(\frac{\partial (n^2)}{\partial p}\right)^2_{c,s}\frac{1}{2\pi}\left(\frac{\Gamma q^2}{(\omega + vq)^2 + (\Gamma q^2)^2} + \frac{\Gamma q^2}{(\omega - vq)^2 + (\Gamma q^2)^2}\right).$$

Γ, the attenuation coefficient of the sound wave, is expressed as

$$\Gamma = \frac{1}{2\rho}\left\{\left(\tfrac{4}{3}\eta_S + \eta_B\right) + (\gamma - 1)\rho D_T + \frac{v^2}{\rho} D\left(\frac{\partial \mu}{\partial c}\right)^{-1}_{p,T}\left[\left(\frac{\partial \rho}{\partial c}\right)_{p,T} + \frac{K_T}{C_p}\left(\frac{\partial \rho}{\partial T}\right)_{p,c}\left(\frac{\partial \mu}{\partial c}\right)_{p,T}\right]^2\right\}.$$

ρ is the mass density, D_T is the thermal diffusivity, D is the mass diffusivity, and K_T is the thermal diffusion ratio. The first term represents the damping of sound by the shear viscosity η_S and the bulk viscosity η_B. Typically, at a scattering angle of 90°, the corresponding linewidth is in the range 500 MHz (3×10^9 rad sec^{-1}). This very high value makes the contributions of the other terms negligible, which corresponds to the coupling with the entropy mode (linewidth $\simeq 5$ MHz) or to the mass diffusion mode (linewidth $\lesssim 5$ kHz). So we can write

$$\Gamma \simeq \frac{1}{2\rho}\left(\tfrac{4}{3}\eta_S + \eta_B\right).$$

Other contributions, such as depolarized lines which cannot be resolved because they are too broad, look like a flat background B (see below). Other contributions such as quasielastic scattering from dust in the sample, etc., add a nearly Dirac function $D\delta(\omega)$ to $S(q,\omega)$.

Finally $S(q,\omega)$ can be put under the following form (Fig. 1):

$$S(q,\omega) = S_1(q,\omega) + S_2(q,\omega) + 2S_3(q,\omega) + D\delta(\omega) + B.$$

III. EXPERIMENTAL

Close to T_c the intensity from the line $S_1(q,\omega)$ strongly increases, giving rise to spurious effects. So we used both a system where $(\partial(n^2)/\partial c)_{p,T}$ is very low and a high-contrast FP spectrometer.

This mixture consists of nitroethane and isooctane, the refractive indices of which are matched within $\sim 10^{-3}$.[19] We already used the very same sample for refractive index[19–21] and depolarized scattering[22] measurements. The purity of nitroethane was better than 99.5%, as verified by chromatography and NMR measurements. The isooctane used had the quality "reference substance for gas chromatography." The isooctane mass fraction was $c = 0.5344 \pm 0.0008$, close to the critical value 0.5350 ± 0.0006.[19] The mixture was frozen

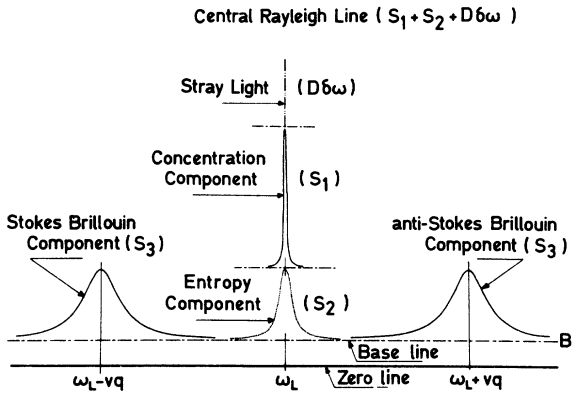

FIG. 1. Schematic Rayleigh-Brillouin spectrum of a binary mixture. In an actual experiment, the three central lines appear as a single apparatus function, and the whole spectrum is periodically repeated with possible overlaps of the Brillouin lines.

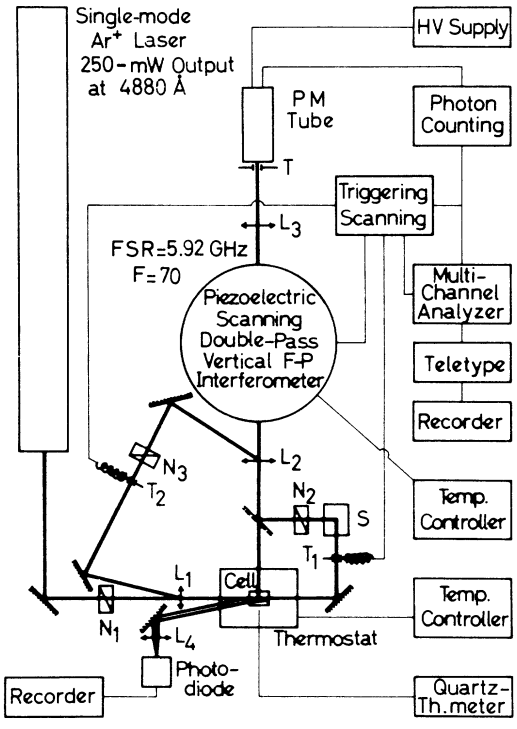

FIG. 2. Experimental setup. N_1, N_2, N_3 are attenuators, L_1–L_4 are lenses. T is a pinhole. When the chopper T_1 is open, the system records an apparatus function from the elastic scatterer S. When T_2 is open, laser light is sent through the interferometer for synchronization. Fringes are formed on the plane of the photodiode by the beams reflected from both walls of the cell.

in liquid nitrogen and sealed under vacuum.

The cell was placed into a thermally stabilized copper oven, itself enclosed in an air-regulated box allowing a thermal stability of $\pm 2 \times 10^{-4}$ K to occur for more than one day, as verified by a quartz thermometer.

Owing to the nearly perfect matching of the refractive indices, no visible opalescence occurs at T_c, and even the meniscus is hardly visible. Therefore, special care was necessary to determine the critical temperature. We set up an experiment as in Ref. 23, where the beam reflected from the input window of the sample interferes with the beam reflected from the output window. This is a very simple, sensitive, and accurate way to determine the refractive index variation. At T_c, due to the phase-separation process, the variation of the refractive index with temperature increases sharply.[19] Moreover, the equilibrium value is reached only after a very long time. This allows us to determine accurately the critical temperature. The value was $T_c = 30.1605 \pm 0.0015\,^{\circ}\mathrm{C}$. The absolute value is accurate only within 0.1 °C.

The light-scattering setup (Fig. 2) is almost the same as in Ref. 24 except for the laser which worked on a single mode with a power of about 250 mW at a wavelength $\lambda = 4880$ Å. Near the critical point, heating by the laser beam was detected in the sample (about 0.5 mK/mW), so the power had to be reduced down to 1 mW.

The mean scattering angle was $90^{\circ} \pm 5'$. The refractive index extrapolated at 4880 Å and 30 °C from Ref. 25 is $n = 1.392 \pm (1 \times 10^{-3})$ (for a complete discussion see below). The mean transfer wave vector is $q = (2.534 \pm 0.002) \times 10^5\ \mathrm{cm}^{-1}$. The aperture angle was about 1°, broadening the Brillouin lines certainly no more than 35 MHz (2.2×10^6 rad sec^{-1}). This is completely negligible with respect to other broadenings, such as the apparatus function (AF) of the spectrometer (see below), as shown by the similarity of the spectra recorded with the full aperture and with the aperture reduced by a factor of 3.

In order to calibrate the intensity, we recorded every 20 sec the elastic light scattered from a solid opalescent medium, used as a standard, which was illuminated by the transmitted beam. The corresponding spectrum looked like an apparatus function. This allows us to know the exact shape of the apparatus function, which can vary in time because of misadjustments, and to automatically correct for the variations of the laser intensity, the transmission of the FP, etc., though we found *a posteriori* that this last factor kept remarkably constant.

The free spectral range (FSR) of the FP was 5.92 ± 0.01 GHz. It was determined by measuring

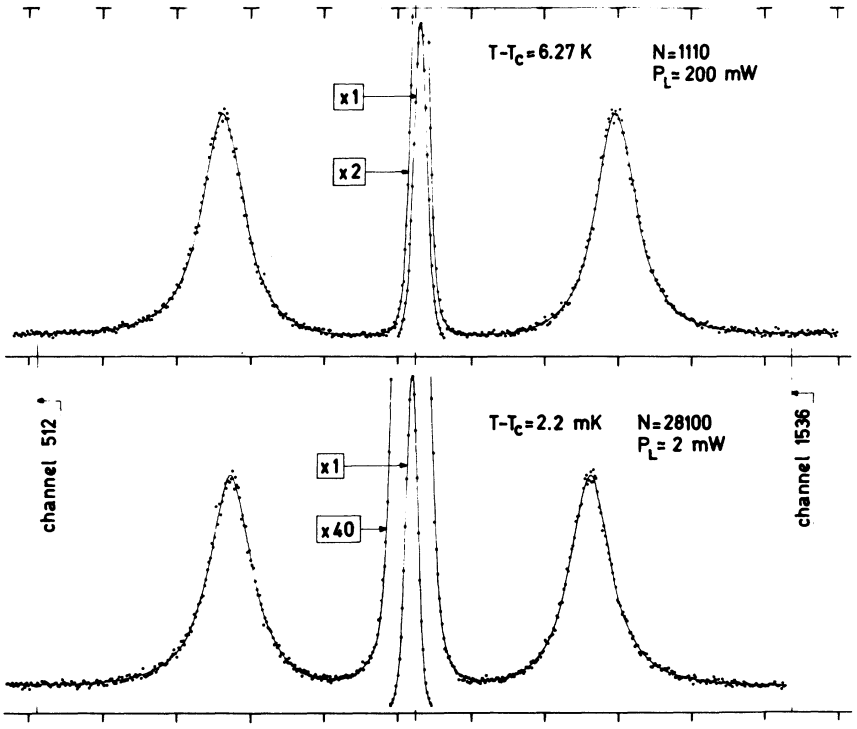

FIG. 3. Two typical spectra. Close to T_c the laser power was reduced to 2 mW, requiring the accumulation of 38 000 scans of 2 sec each. Far from T_c, with 200 mW, 1100 scans are enough to obtain a good signal-to-noise ratio.

the spacing between the plates by means of a cathetometer. The finesse was typically 70, corresponding to a half-width at half-height of the apparatus function of 50 MHz, and the contrast was found to be better than 10^6. The adjustments were stable enough to allow recording during 24 h or more, but the typical duration time of a recording was 1 or 2 h, except near T_c where the laser power was considerably reduced, as explained above.

Figure 3 shows two typical spectra obtained far from T_c (6.27 K) or very close to T_c (2.2 mK). The ratio of the central peak height to the Brillouin height varies typically from 2–40 (that of the integrated intensities from 0.3–6.5). The resolution of 50 MHz merges the entropy and concentration lines into an apparatus function, but the Brillouin linewidth is clearly evidenced. The baseline is different from zero, due in part to the unresolved broad depolarized lines.

The parameters, which can be determined at each temperature, are the shift, linewidth, and intensity of the Brillouin lines, the intensity of the central peak, and the intensity of the baseline (Table I). The experimental spectra are the convolution of $S(q, \omega)$ by the apparatus function. We analyzed the recordings as follows: Only a few spectra, each considered as typical of a given $T - T_c$ range, were analyzed using the apparatus function recorded simultaneously. We used a program of statistical refining due to M. Tournarie,[26] which allows the determination of the above quantities. But this kind of analysis is long and expensive, and we found it possible to simplify this analysis by some practical considerations. The background was deduced from the lowest points of the spectrum and then the heights h_B, h_R and apparent widths at half-height $2\Gamma^*$, $2\Gamma_R^*$ of the Brillouin and Rayleigh lines were measured. The true Brillouin linewidth is then given by

$$2\Gamma = 1.35(2\Gamma^* - 2\Gamma_R^*)$$

and the intensities of the Brillouin and Rayleigh lines by

$$I_R = 1.12\, h_R 2\Gamma_R ,$$

$$I_B = 0.96\pi h_B 2\Gamma \quad \text{(average of both lines)} .$$

The uncertainties are 0.5% for the Brillouin shift, 3% for the intensities, and range from 3–8% for the Brillouin linewidth, the larger value applying far from T_c, where the Brillouin lines of consecutive orders overlap.

TABLE I. Measured values of the Brillouin shift ($\Delta\nu$) and linewidth (Γ) and the intensities of the Rayleigh line (I_R), the Brillouin lines ($2I_B$), and the background (B). These intensities are referred to as the elastic scatterer (I_{AF}) so that their scale is arbitrary.

N	$T-T_c$ (°C)	$\Delta\nu$ (GHz)	Γ (MHz)	$\frac{I_R}{2I_B}$	$\frac{2I_B}{I_{AF}}$	$\frac{I_R}{I_{AF}}$	B
01	60.64	3.4185	241.9	0.270	1.92	0.72	0.68
02	52.44	3.561	241.9	0.265	1.85	0.685	0.72
03	47.64	3.647	249.8	0.270	1.72	0.65	0.69
04	43.34	3.708	253.7	0.270	1.50	0.57	0.61
05	39.14	3.7885	273.2	0.270	1.63	0.615	0.75
06	36.64	3.838	265.4	0.275	1.73	0.67	0.83
07	34.74	3.8665	277.1	0.280	1.50	0.59	0.72
08	29.34	3.9625	284.9	0.280	1.47	0.58	0.76
09	23.64	4.071	300.5	0.275	1.23	0.475	0.63
10	18.14	4.1555	304.4	0.285	1.57	0.63	0.93
11	13.74	4.254	312.2	0.290	1.25	0.52	0.85
12	9.95	4.3065	327.8	0.30	1.18	0.50	0.82
13	6.2675	4.381	331.7	0.305	1.17	0.50	0.86
14	4.25	4.410	339.5	0.33	1.20	0.555	0.88
15	3.968	4.419	343.4	0.35	1.21	0.60	1.03
16	3.7345	4.430	339.5	0.36	1.17	0.59	0.96
17	2.83	4.435	351.2	0.37	1.13	0.585	0.97
18	2.54	4.4555					
19	2.03	4.446	343.4	0.445	1.11	0.69	0.92
20	1.7345	4.465	351.2	0.46	1.08	0.70	
21	1.695	4.467	351.2	0.47	1.11	0.735	0.93
22	1.18	4.465	347.3	0.57	1.20	0.96	0.89
23	1.135	4.4755					
24	0.84	4.479	351.2	0.69	1.06	1.02	0.87
25	0.755	4.4755	343.4	0.755	1.09	1.16	0.85
26	0.7455	4.482	351.2	0.745	1.17	1.22	1.08
27	0.6895	4.477	347.3	0.81	1.23	1.39	1.00
28	0.6203	4.486	359.0	0.90	1.12	1.42	1.16
29	0.5747	4.482	359.0	0.93	1.04	1.35	0.82
30	0.565	4.482					
31	0.560	4.482	351.2	0.945	1.12	1.49	0.93
32	0.469	4.483	347.3	1.07	1.19	1.78	0.95
33	0.4325	4.488	355.1	1.14	1.28	2.04	1.20
34	0.356	4.485	343.4	1.30	1.05	1.92	0.96
35	0.28	4.482					
36	0.2762	4.493	347.3	1.60	1.15	2.54	1.17
37	0.270	4.495	355.1	1.625	1.12	2.56	0.93
38	0.2655	4.492	359.0	1.76	1.16	2.86	0.89
39	0.2433	4.493	359.0	1.86	1.07	2.79	0.86
40	0.2415	4.486	347.3	1.73			0.97
41	0.2375	4.493	355.1	1.94	1.15	3.13	0.87
42	0.2185	4.4915	347.3	2.00	1.16	3.26	0.86
43	0.2180	4.478	355.1	1.95			1.04
44	0.1985	4.4955	359.0	2.20	1.11	3.42	0.85
45	0.1970	4.492	362.9	2.16	1.12	3.40	0.90
46	0.1918	4.494	347.3	2.25	1.09	3.45	0.81
47	0.1765	4.486	355.1	2.40	0.96	3.22	0.97
48	0.1698	4.492	359.0	2.43	1.07	3.66	0.85
49	0.1673	4.495	355.1	2.57	1.10	3.97	0.86
50	0.1568	4.493	351.2	2.65	1.09	4.05	0.85
51	0.1490	4.486	351.2	2.60	0.99	3.60	0.90
52	0.1375	4.496	347.3	2.75	1.06	4.10	1.12
53	0.1315	4.490	351.2	2.84	1.11	4.40	0.89
54	0.1213	4.4845	359.0	2.85	1.19	4.75	1.10
55	0.1195	4.489	355.1	3.25	1.14	5.20	1.12
56	0.1114	4.4915	359.0	3.20	1.13	5.05	1.11
57	0.1018	4.497	362.9	3.50	1.09	5.25	1.26
58	0.092	4.486	355.1	3.60	1.13	5.7	1.21
59	0.079	4.499	351.2	4.00	1.11	6.25	1.26
60	0.070	4.490	347.3	4.20	1.09	6.4	1.10
61	0.063	4.4955	355.1	4.70	1.12	7.4	1.20
62	0.059	4.493	351.2	4.40	1.11	6.9	1.08
63	0.047	4.492	355.1	4.75	1.17	7.8	1.12
64	0.035	4.495	355.1	5.50	1.06	8.2	1.07
65	0.026	4.491	343.4	5.90	1.11	9.2	1.10
66	0.024	4.495	362.9	5.85	1.10	9.0	1.12
67	0.018	4.487	355.1	6.05	1.10	9.3	1.09
68	0.0125	4.494	359.0	6.50	1.04	9.5	1.02
69	0.0022	4.489	351.2	6.50	1.11	10.1	1.10
70	0.0010	4.496	359.0	7.50	1.15	12.0	1.15

IV. RESULTS AND DISCUSSION

A. Hypersound velocity

Primarily we have determined the hypersound velocity of the pure components. The setup which consisted of 2 FP in tandem allowed the velocity to be determined at two frequencies: High frequency with only the plane FP (back scattering $\theta \simeq 150°$, shift $\Delta\omega \simeq 5$ GHz, and "low" frequency with the plane FP used as a filter and a confocal FP used as an analyzer (forward scattering $\theta \simeq 25°$, $\Delta\omega \simeq 1$ GHz). The velocities $v = 2\pi\Delta\omega/q$ are listed in Table II, where they can be compared to ultrasonic measurements at 24 MHz. The uncertainty is typically 1%, and is due chiefly to the uncertainty on q (see below). A weak positive dispersion can be deduced, which is commonly found in liquids. This dispersion was already detected with ultrasonic measurements.[14]

The nitroethane-isooctane mixture is ideal within 1% with respect to the volume additivity.[20] We consider the relationship $v^2 = (\rho\beta_s)^{-1} = (\partial\rho/\partial p)^{-1}_{s,c}$ and the volume additivity, which lead to the density formulation $\rho^{-1} = c\rho_1^{-1} + (1-c)\rho_2^{-1}$ with c the mass fraction of isooctane. Subscripts 1 and 2 refer to, respectively, isooctane and nitroethane. In this case, it is straightforward to deduce the ideal velocity v_{id} from the velocity of each component v_1 and v_2:

TABLE II. Velocity measurements from hypersonic and ultrasonic techniques near the critical point of binary mixture.

Systems	FP technique	Hypersonic measurements: Frequency measurement (GHz)	Hypersonic measurements: Temperature measurement (°C)	Hypersonic measurements: Linear variation v_c (m sec^{-1})	Hypersonic measurements: Linear variation dv/dT (m sec^{-1} K^{-1})	Hypersonic measurements: Critical anomaly	Ultrasonic measurements: Critical anomaly	Ultrasonic measurements: Temperature measurement (°C)	Ultrasonic measurements: Linear variation v_c (m sec^{-1})	Ultrasonic measurements: Linear variation dv/dT (m sec^{-1} K^{-1})	Ultrasonic measurements: Frequency measurements (MHz)	Dispersion
nitroethane	2 FP[a]	5.7	23 ± 0.5	1320 ± 50[a]	?			32	1262[b]	?	24	negligible[b] up to 4 GHz
	tandem	0.789	23 ± 0.5	1320 ± 10[a]								
isooctane	2FP[a]	4.8	23 ± 0.5	1110 ± 50[a]	?			11	1050[b]	?	24	weak after[b] 1 GHz
	tandem	1.15	23 ± 0.5	1120 ± 10[a]								
nitroethane + isooctane	1 pass[c]	3.42	30.16[d]	1088 ± 1[e]	−3.8 ± 0.5[e]	No (± 1%)	No (± 0.2%)	30.16[d]	1088 + 2[d,g]	−4.0 ± 0.2[g]	10.24	?
				1088 ± 10[f]	−3.8 ± 0.5[f]							
	2 pass[a]	4.49	30.16[a]	1115.42 ± 0.18[e]	−4.04 + 0.02[e]	No (± 0.5%)						
				1115 ± 10[f]	−4.04 ± 0.05[f]							
	ideal value[a]			1146 ± 10						1077		
nitrobenzene	1 pass[h]	7.59	20.20	1548 ± 10[f]	−5.8 + 1.3[l]							
n-hexane	1 pass[h]	4.82	20.20	1110 ± 10[f]	−4.9 ± 1.3[l]							
nitrobenzene + *n*-hexane	1 pass[j]	3.94	20.00	1226 ± 12[j]	−4.7 ± 1[l]	Yes: −10% at $T-T_c=0.1$ °C	Yes (−0.5%)	20.6	1215 ± 2[k]	−3.64 ± 0.05[k]	15	?
	1 pass[h]	5.59	20.20	1229 ± 12[f]	−4.1 ± 1[l]	Yes: −10% at $T-T_c=0.1$ °C						
	2 pass[i]	4.63	20.90	1170 ± 12[f]	−4.0 ± 0.5[l]	No (± 1%)						
	ideal value[a]			1135 ± 10								
nitroethane 3-methylpentane	2FP[o] tandem	~5	26.38			No						
water + triethy-amine	1 pass[m]	5	18	1385 ± ?	~ −11	Yes: +10% at $T-T_c=0.1$ °C	Yes: (−1%)		1330[n]	−11.5[n]	0.6	

[a] This work.
[b] Reference 14.
[c] Reference 16.
[d] For sake of comparison, we have extrapolated the value at the same temperature $T_c=30.16$ °C. The value found in c was $T_c=30.91$ °C. The isooctane mass fraction in c is 0.503, here it is 0.5344. The influence is weak: $dv/dc \sim -6$ m sec^{-1}.
[e] The uncertainty concerns the relative values directly deduced from the Brillouin shift.
[f] Absolute value and corresponding error.
[g] Reference 15.
[h] Reference 11 (0.42 mole fraction of nitrobenzene).
[i] Reference 13. Same sample as in h.
[j] Reference 9 (0.40 mole fraction of nitrobenzene). With $dv/dc \simeq 8.4$ m sec^{-1}, the velocity becomes 1218 m sec^{-1} at 0.42 mole fraction.
[k] Reference 8.
[l] We have taken into account the thermal variation of the refractive index (see text).
[m] Reference 7.
[n] Reference 6.
[o] Reference 12.

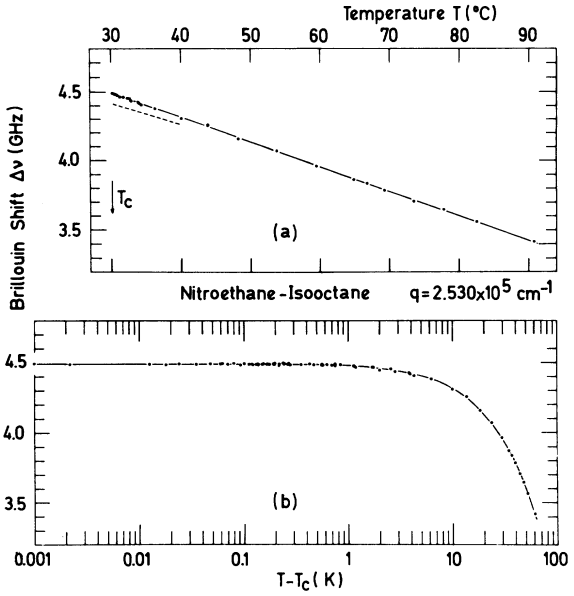

FIG. 4. Plot of the Brillouin shift versus the temperature in linear and semilog coordinates. No anomaly has been detected. The dotted line shows the results of Aref'ev *et al.* (Ref. 16).

$$(\rho v_{id})^{-2} = c(\rho_1 v_1)^{-2} + (1-c)(\rho_2 v_2)^{-2} .$$

The value found for the nitroethane-isooctane system is in Table II, together with that found for the nitrobenzene–*n*-hexane mixture, where hypersonic measurements are available in the literature. In both cases, comparison with experimental data shows relatively good agreement, within 4–5%.

The Brillouin shift of the mixture has been obtained with an accuracy better than 0.5%, this uncertainty taking into account the nonlinearity of the FP scanning. Figure 4 shows unambiguously that within a 0.5% precision, no anomaly of the shift can be detected in the range $T - T_c = 1$ mK–60 K, ($t = 3.3 \times 10^{-6}$–0.2). Only a linear dependence is seen, which is compatible with the hypersonic data of Aref'ev *et al.*[16] (no anomaly within 1%) and the ultrasonic measurements of Anisimov *et al.*,[15] which were both performed with the nitroethane-isooctane mixture. There is also agreement with the Brillouin measurements of Kruer *et al.*[12] on the nitroethane–3-methylpentane system, and with Wang's[13] data on the nitrobenzene–*n*-hexane mixture. Ultrasonic experiments on the last mixture by d'Arrigo *et al.*[8] have shown only a 0.5% negative anomaly near T_c.

On the other hand, our results contrast with Brillouin-shift measurements in the water + triethylamine and nitrobenzene + *n*-hexane mixtures reported by Aref'ev *et al.*[7,10] and Chen *et al.*[11] where, respectively, a +10% and −10% shift anomaly has been observed close to T_c. Let us notice, however, that the FP technique used (single pass) is not well adapted to these opalescent mixtures, as we have discussed above, so these data cannot be regarded as conclusive.

From the Brillouin shift $\Delta\nu$, it is straightforward to obtain the hypersound velocity $v = 2\pi\Delta\nu/q$. The shift, being a linear function of T, can be written as

$$\Delta\nu = \Delta\nu_c + \left(\frac{d(\Delta\nu)}{dT}\right)(T - T_c) .$$

The critical anomaly of the refractive index has been found negligible in this mixture.[20,21] We can therefore write

$$q = q_c\left[1 + \frac{1}{n_c}\left(\frac{dn}{dT}\right)_p (T - T_c)\right]$$

so that

$$v(T) = v(T_c) + (T - T_c)\left[\frac{2\pi}{q_c}\frac{d(\Delta\nu)}{dT} - \frac{v_c}{n_c}\left(\frac{dn}{dT}\right)_p\right].$$

The values of n and $(dn/dT)_p$ have been accurately determined in Refs. 21 and 25 for the wavelength $\lambda = 6328$ Å. Since we used $\lambda = 4880$ Å, we had to evaluate the dispersion correction. An order of magnitude for the dispersion correction of the refractive index of the mixture can be evaluated by comparison with the data for pure components.[27] We have estimated the refractive index at 30 °C and 4880 Å to $n = 1.392 \pm 0.001$.

The wavelength dependence of $(dn/dT)_p$ is certainly very weak and we can adopt the value measured at 6328 Å: $(dn/dT)_p = -(4.936 \pm 0.002) \times 10^{-4}$ K^{-1}. Apart from the determination of the shift, uncertainties about the absolute value of the velocity arise from uncertainties in the free spectral range (0.15%) and the transfer wave vector q (0.2%). The total uncertainty is therefore about 1%.

The values of the velocity have been listed in Table II, together with other data concerning ultrasonic or hypersonic measurements in the same system and in two other binary mixtures. For these mixtures we have determined the velocity and its thermal derivative as above. When necessary (nitroethane-isooctane by Aref'ev *et al.*,[16] we have taken into account the small corrections due to the differences in critical concentrations or critical temperatures (see the caption of Table II). The agreement between ultrasonic and hypersonic measurements is good and our data show a very small positive dispersion (+2.5% ± 1%), contrary to other measurements by Aref'ev *et al.* (0 ± 1%).[16]

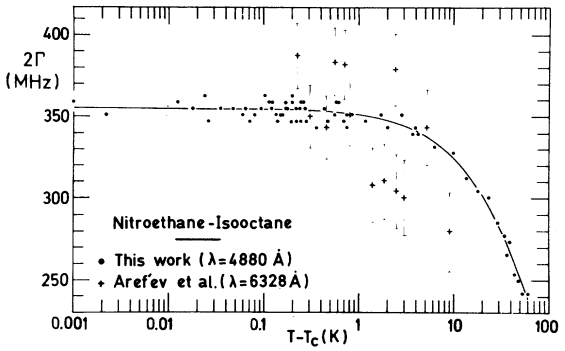

FIG. 5. Brillouin full linewidth 2Γ versus the logarithm of $T-T_c$. The behavior is regular and follows an Arrhenius law (solid curve). Also shown are the data of Ref. 16.

B. Hypersound attenuation

The true full linewidth 2Γ of the Brillouin lines, deduced from the experimental spectrum as explained above, is shown in Fig. 5 versus $T-T_c$ (semilog plot). The accuracy is typically 3%, which allows the thermal variation to be clearly evidenced in a wide range of $T-T_c$ (1 mK–60 K). Also are reported the data of Aref'ev *et al.*[16] from the same mixture, taking into account the difference in the q wave vectors. Although the precision of these data is rather low, they appear to be in agreement.

As for the Brillouin shift, no anomaly in the vicinity of the critical point is visible. This is in contradiction with the data on the nitrobenzene–*n*-hexane mixture in which a critical broadening of the linewidth has been seen. Chen *et al.*[11] used a single-pass FP and the results might have been influenced near T_c by the strong opalescence of the system. Wang,[13] using a double-pass FP, reported also some critical broadening of the linewidth, although he was not able to measure the effect.

It is interesting to note that a strong absorption of the sound is commonly observed at a low frequency near T_c. This is due to the coupling between the sound modes (frequency ω_S) and the critical concentration modes (frequency ω_c). Indeed, an adiabatic pressure fluctuation generates a temperature fluctuation which has a strong influence near T_c on the concentration fluctuation. This coupling is efficient only if the pressure fluctuations have enough time to "feel" the concentration fluctuations, i.e., if $\omega_S \lesssim \omega_c$. Since ω_c is low, ($\omega_c/2\pi < 0.01$ MHz), Brillouin experiments cannot be concerned with this kind of broadening. It is well established now that this ultrasound absorption is strongly frequency dependent, and that no effects are visible for frequencies higher than $\simeq$0.1 GHz. We therefore, expect no contributions from this coupling in a Brillouin experiment working at $\simeq$5 GHz.

Sound absorption arises mainly from the shear and bulk viscosities. The shear viscosity η_S exhibits a critical behavior governed by the exponent $y_\eta \simeq 0.04$[28]:

$$\eta_S = \eta_S^{\text{reg}} t^{-y_\eta} .$$

η_S^{reg} is the regular part of the viscosity, which usually behaves as an Arrhenius law with an activation energy E. Therefore, $\eta_S = \eta_0 t^{-y_\eta} \exp[E/T_c(1+t)]$. As for the sound absorption, the critical part of the viscosity is due to the coupling between the viscous modes and the critical-concentration modes, and the same relaxation effect with frequency is expected. This has been verified by shear flow measurements.[29–31]

Concerning the bulk viscosity η_B, a strong $T-T_c$ dependence is expected[2,4,5]; this approach is quite similar to the direct study of the coupling between the sound mode and the concentration mode.[1,3] The same arguments as above concerning the frequency dependence of the coupling lead to the conclusion that the bulk viscosity should not have any critical anomaly at the Brillouin frequencies.

It is therefore logical to relate the Brillouin linewidth to the regular part of the viscosities:

$$\Gamma q^2 = \frac{q^2}{2\rho}\left(\tfrac{4}{3}\eta_S^{\text{reg}} + \eta_B^{\text{reg}}\right) .$$

We tried the following fits (see Table III):

(i) $\Gamma q^2 = X_2 \exp(X_1/T)$,

assuming the same Arrhenius temperature dependence for both η_S and η_B. The fit of the data is good, but the activation energy $X_1 = 751 \pm 13$ K corresponds to the lower limit of the activation energy obtained from the shear viscosity measurements $E = 920 \pm 180$ K.[22] This means that the bulk viscosity η_B should exhibit a temperature dependence weaker than η_S. So we tried the fit as follows.

(ii) $\Gamma q^2 = X_2 \exp(X_1/T) + X_3$,

with the restriction $X_1 = E = 920 \pm 180$ K, but the results show that the best fit is obtained with a poor determination of X_2 and X_3, which suggests that the temperature dependence of η_B, although weak, cannot be neglected. The 3rd fitting function was the following:

(iii) $\Gamma q^2 = X_2 \exp(X_1/T) + X_3 + X_4 T$,

where we have added a term linearly dependent on T.

With all parameters free or with $X_1 = E$ imposed as above, X_4 is undetermined. But the lower limit of X_2 is almost compatible with the value deduced

TABLE III. Fit of the half-linewidth of Brillouin lines to $\Gamma q^2 = X_2 \exp(X_1/T) + X_3 + X_4 T$. We have assumed $\Gamma q^2 = (q^2/2\rho)[(4/3)\eta_S^{reg} + \eta_B^{reg}]$ (see text). From shear flow measurements (Ref. 22) $\eta_S = \eta_0 \exp(E/T)\{[(T - T_c)/T_c]^{-y_\eta}\}$ with $\eta_0 = 2.18 \times 10^{-4} P$, $E = (920 \pm 180)$ K, and $y_\eta = 0.045 \pm 0.013$. We have used $\rho = 0.821$ g cm^{-3} at $T = 303$ K (Ref. 20) and $q = 2.53 \times 10^5$ cm^{-1} (see text). Q is a statistical quality coefficient (=1 if the uncertainties are randomly distributed, =0 if not).

X_1 (K)	X_2 (MHz)	X_3 (MHz)	X_4 (MHz K^{-1})	Q	$\sigma(\Gamma)$ (%)	Remarks
751 ± 13	14.8 ± 0.7	(0) imposed	(0) imposed	0.875	1.4	X_3, X_4 imposed to (0)
967 ± 14	5.9 ± 3.6	33.4 ± 17	(0) imposed	0.873	1.4	X_1 imposed to (920 ± 180) K
1134 ± 211	2.8 ± 2.5	90 ± 62	−0.10 ± 0.13	0.872	1.4	all free parameters
1000 ± 120	4.7 ± 2.4	77 ± 57	−0.10 ± 0.11	0.872	1.4	X_1 imposed to (920 ± 180) K

from the regular shear viscosity $X_2 = (q^2/2\pi)(2\eta_0/3\rho) = 1.80$ MHz (values from Table III caption).

From another point of view, these linewidth data can be regarded as measurements of the viscosity, and it seems interesting to compare these results with other indirect viscosity determinations, such as the linewidth of the molecular reorientation spectrum (depolarized scattering), which has been done in the same critical mixture.[22] In Table IV the data in terms of frequency-dependence viscosity for several mixtures are reported, using Brillouin or depolarized scattering, Kerr effect, and the usual shear flow viscosimeter determination. As expected the low-frequency measurements exhibit a divergence, which nevertheless levels off when the frequency of the measurement becomes comparable to the concentration fluctuation frequency.[29-31] As far as the nitroethane-isooctane system is concerned, only the regular behavior is detected for frequencies 5 and 100 GHz. This is well explained by relaxation phenomena as noticed above. The nitrobenzene–*n*-hexane mixture shows a different behavior, a diverging part being detected for frequencies up to 15 GHz. However, this system is very opalescent, and one could consider the data from Ref. 11 as not very reliable since they were obtained using a single-pass FP. The same difference of behavior has been noticed in the study of the reorientation motion, two techniques, double-pass FP,[32] and optical Kerr effect[33] with a picosecond laser giving the same results, although with somewhat different reorientation times (respectively, 10 and 15 GHz).

This rather puzzling situation suffers from a lack of data concerning other binary mixtures, which prevents any further considerations being made.

C. Brillouin intensity

As explained above, the ratio of the integrated spectral intensity of the Brillouin line $I_B = \int_{-\infty}^{\infty} S_3(\omega)\, d\omega$ to the intensity of the FP apparatus function allows the relative variation of I_B to be measured versus temperature. This is shown in Fig. 6, where a smooth linear variation with T is visible. If the difference between the temperature variation of the scattering volumes of the AF and the mixture are neglected, the intensity I_B must vary as

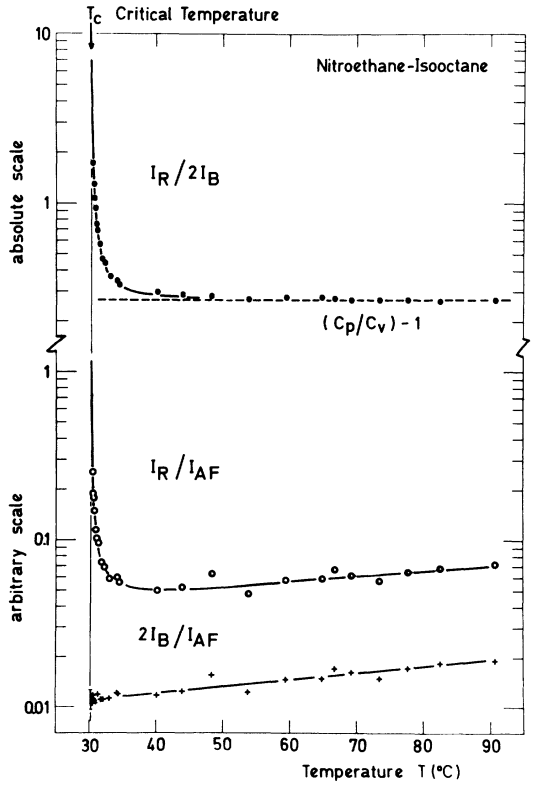

FIG. 6. Different ratios of the intensities of the Rayleigh line I_R, the Brillouin lines $2I_B$, and the intensity standard I_{AF}. The horizontal asymptote of $I_R/2I_B$ shows that strong light is negligible.

TABLE IV. Shear viscosity measurements by different methods and at various frequencies. As typical frequency in the shear flow viscosimeter experiments it has been taken the shear rate; $[t=(T-T_c)/T_c$ and $y_\eta \simeq 0.04]$.

System	Optical Kerr effect Frequency (GHz)	Behavior	Molecular reorientation Frequency (GHz)	Behavior	Brillouin spectrum Frequency (GHz)	Behavior	Shear flow viscometer Frequency (GHz)	Behavior
Nitroethane + Isooctane			100[a]	regular × exp(E/T)	4.5	regular × exp(E/T)	100[b]	regular × divergent $t^{-y_\eta}\exp(E/T)$
Nitrobenzene + *n*-hexane	15[c]	regular × divergent $t^{-y_\eta}\exp(E/T)$	10[d]	regular × divergent $t^{-y_\eta}\exp(E/T)$	5.5[e]	regular × divergent $t^{-y_\eta}\exp(E/T)$	100[f]	regular × divergent $t^{-y_\eta}\exp(E/T)$

[a] Reference 22.
[b] This work.
[c] Reference 33.
[d] Reference 32.
[e] Reference 11.
[f] Reference 30.

$$k_B T \beta_s \left(\frac{\partial(n^2)}{\partial\rho}\right)^2_{T,c}.$$

Using the definition of β_s and the well-known relationship

$$\beta_s = (\rho v^2)^{-1}, \quad I_B \propto T\left(\rho\frac{\partial(n^2)}{\partial\rho}\right)^2_{T,c}\Big/\rho v^2.$$

An order of magnitude of the variation is given by

$$\frac{1}{I_B}\left(\frac{dI_B}{dT}\right) \simeq \frac{1}{T_c} - \frac{1}{\rho}\left(\frac{\partial\rho}{\partial T}\right)_p - \frac{2}{v_c}\frac{dv}{dT} + \frac{4n}{n^2-1}\left(\frac{dn}{dT}\right)_p,$$

where the Rocard relation $[\rho\,\partial(n^2)/\partial\rho]^2_T = (n^2-1)^2$ was assumed[18] for simplicity (the Einstein or Yvon-Vuks formulations do not change the results appreciably). Each term is known, except $(1/\rho)(\partial\rho/\partial T)_p$, which can be estimated as $(-1.2\times10^{-3})\ \mathrm{K}^{-1}$ when looking at each component,[25] and one finally obtains $(1/I_B)(dI_B/dT) \simeq 10^{-2}\ \mathrm{K}^{-1}$, which agrees well with the data as shown in Fig. 6.

D. Background intensity

The recorded spectra show a non-negligible baseline due to broad lines, which cannot be resolved in the free spectral range of the FP. One component of this background is the scattering due to the anisotropy of the nitroethane molecules,[22] but other mechanisms (Raman, collision-induced, etc.) also contribute.

E. Rayleigh intensity: Rayleigh-Brillouin ratio

The Rayleigh intensity measures the nonresolved contributions from stray light, entropy fluctuations, and (critical-) concentration fluctuations. We first checked that the stray light, which is expected to have no temperature variation, was negligible. Stray light is exhibited far from T_c, where concentration fluctuations are negligible. Figure 6 shows that, far from T_c, the Rayleigh intensity normalized to the FP apparatus function varies as the Brillouin intensity, which proves that the stray light is effectively negligible versus the entropy contribution so that the ratio Rayleigh-Brillouin measures the ratio entropy-Brillouin, i.e., the Landau-Placzek ratio. It is well known that this ratio is equal to $(C_p/C_v)-1=\gamma_0-1$. In critical mixtures C_v is regular while C_p is the sum of a regular part and a diverging part, with the exponent $\alpha \simeq 0.1$. However, refractive-index measurements[20] have shown that the amplitude of the diverging part is very small in this mixture so that C_p can be considered as regular here, and the ratio γ_0 as independent of the temperature. The low value found $\gamma_0 = 1.27$ is a final check of the smallness of the stray light.

We then fitted the experimental Rayleigh-Brillouin ratio taking into account only the two contributions $S_1/2S_3$ and $S_2/2S_3$ (see Figs. 1 and 7):

$$\frac{I_R}{2I_B} = \left(\frac{\left(\frac{\partial(n^2)}{\partial c}\right)^2_{p,T}}{\left(\rho\frac{\partial(n^2)}{\partial\rho}\right)^2_{T,c}}\frac{\rho v^2}{\left(\frac{\partial\mu}{\partial c}\right)^0_{p,T}}\, t^{-\gamma} G(q,\xi)\right) + (\gamma_0 - 1).$$

As we have stressed above, this ratio is independent of the light-scattering theories. For simplic-

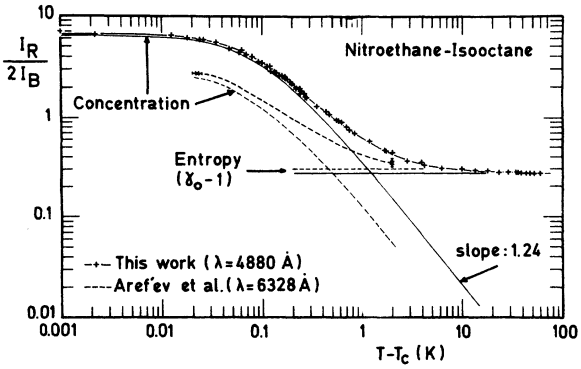

FIG. 7. Rayleigh-Brillouin ratio versus $T-T_c$ (log-log plot) showing the different contributions to the Rayleigh peak (this work and Ref. 16).

ity we shall use the Einstein formulation, where the factors $(\partial(n^2)/\partial c)_{p,T}$ and $(\partial(n^2)/\partial\rho)_{T,c}$ are mathematical derivatives and can be calculated using the Lorentz-Lorenz formula.

We know $(\partial n/\partial c)_{p,T}$ at $T\sim 30$ °C and $\lambda = 6328$ Å,[34]

$$\left(\frac{\partial n}{\partial c}\right)_{p,T} = (1.34 \pm 0.04) \times 10^{-3},$$

the dispersion correction can be estimated from the literature,[27]

$$\left(\frac{\partial n}{\partial c}\right)_{p,T}(4880\text{ Å}) = \left(\frac{\partial n}{\partial c}\right)(6328\text{ Å}) + (1.2 \pm 0.2) \times 10^{-3}$$
$$= (2.54 \pm 0.24) \times 10^{-3},$$

while the temperature dependence can be obtained by a straightforward application of the Lorentz-Lorenz theory and the data[20]

$$\frac{\partial n_1}{\partial T} = -4.961 \times 10^{-4}\ \text{K}^{-1},$$

$$\frac{\partial n_2}{\partial T} = -4.774 \times 10^{-4}\ \text{K}^{-1}.$$

We finally get

$$\frac{1}{\left(\frac{\partial(n^2)}{\partial c}\right)_{p,T}} \frac{\partial}{\partial T}\left(\frac{\partial(n^2)}{\partial c}\right)_{p,T} \simeq 7.7 \times 10^{-3}\ \text{K}^{-1}.$$

The evaluation of $\partial n/\partial\rho$ is not accurate if we differentiate the Lorentz-Lorenz formula, and it is better to calculate this ratio from its value in each component.[25] This leads to

$$\rho\left(\frac{\partial(n^2)}{\partial\rho}\right)_{T,c} = 2n \frac{\left(\frac{\partial n}{\partial T}\right)_{p,c}}{\frac{1}{\rho}\left(\frac{\partial\rho}{\partial T}\right)_{p,c}} = 1.14 \pm 0.05,$$

the thermal variation of which can be easily evaluated to $-2 \times 10^{-3}\ \text{K}^{-1}$. The factor ρv^2 exhibits also a T dependence, which can be easily estimated from the above results:

$$\frac{1}{\rho v^2}\frac{d}{dT}(\rho v^2) = -8.2 \times 10^{-3}\ \text{K}^{-1}.$$

$G(q,\xi)$ is the critical contribution of concentration fluctuations, and can be written under the following form, valid within 1% in the range $q\xi = (20 - 5 \times 10^{-4})$[35] [our experiment covers the range $q\xi = (20 - 2 \times 10^{-2})$].

$$G(q,\xi) = [1 + (\alpha_1 q\xi)^2]^{-(1-\eta/2)} + [1 + (\alpha_2 q\xi)^2]^{-\Omega} - [1 + (\alpha_3 q\xi)^2]^{-\Sigma},$$

with $\alpha_1 = 1.040\,056$, $\alpha_2 = 1.058\,947$, $\alpha_3 = 1.053\,932$, $\eta = 0.0315$, $\Omega = 1.554\,213$, $\Sigma = 1.627\,419$. We recall that $\xi = \xi_0[(T - T_c)/T_c]^{-\nu}$.

Finally, the experimental data had to be compared with the following temperature variations:

$$\frac{I_R}{2I_B} = \left[A_c[1 + m(T - T_c)]\left(\frac{T - T_c}{T_c}\right)^{-\gamma} G(q,\xi)\right] + (\gamma_0 - 1),$$

where

$$A_c = \frac{\left[\left(\frac{\partial(n_c^2)}{\partial c}\right)_{p,T}\right]^2}{\left(\rho\frac{\partial(n^2)}{\partial\rho}\right)^2} \frac{\rho_c v_c^2}{\left(\frac{\partial\mu}{\partial c}\right)^0_{p,T}}$$

and $m = 1.1 \times 10^{-2}\ \text{K}^{-1}$. The subscript c means that the value is taken at T_c. The coefficients A_c, ξ_0, ν, γ, and γ_0 are considered as free parameters.

First we have checked that the value of m does not influence the results very much; with (m) set to different values between $-1.6 \times 10^{-3}\ \text{K}^{-1}$ and $+1.6 \times 10^{-2}\ \text{K}^{-1}$, the values of the above parameters did not change within 0.5%, which was within the uncertainties.

Second, with all parameters free, the determination of the amplitude ξ_0 is strongly correlated with ν, as well as A_c with γ, which prevents accurate independent determinations (Fig. 8 reports the values found for ξ_0 as a function of ν, and A_c as a function of γ, for about the same quality of the fit). We thus fixed the exponents at their expected values in binary mixtures (Refs. 36 and 37) $\gamma = 1.2402 \pm 0.0009$, $\nu = 0.6300 \pm 0.0008$. The results of the fit are in Table V.

The values found lead to the following remarks.

i. The correlation length amplitude ξ_0. The uncertainty on ξ_0 is in fact slightly bigger than deduced from the fit, since the true variable is the product $q\xi_0$. Therefore,

$$\xi_0 = 2.42 \pm 0.04\text{ Å}.$$

ii. The Landau-Placzek ratio $(\gamma_0 - 1)$. The value found for the ratio $C_p/C_v = \gamma_0 = 1.2702 \pm 0.0009$ is

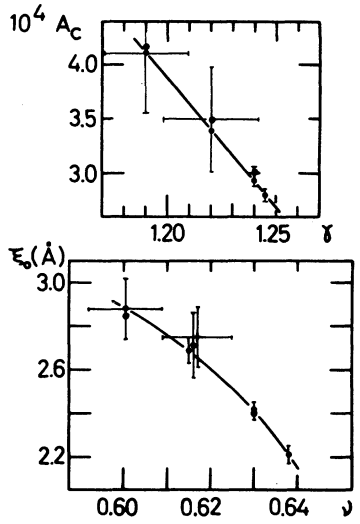

FIG. 8. "Best" values of the couples of correlated variables (A_c, γ) and (ξ_0, ν). It has been necessary to fix the values of the critical exponents to their universal values to determine accurately the amplitudes A_c and ξ_0.

usual in liquids. The comparison with the data of Ref. 16 (see also Fig. 7), where the value 1.30 was found, gives a satisfactory agreement.

iii. The amplitude $(\partial\mu/\partial c)^0_{\rho,T}$ *and the universal amplitude ratio* $R_\xi^+ R_c^{-1/3}$. From the value A_c we can infer

$$\left(\frac{\partial \mu}{\partial c}\right)^0_{\rho,T} = \left(\frac{(\partial(n_c^2)/\partial c)_{\rho,T}}{\rho(\partial(n_c^2)/\partial\rho)}\right)^2 \frac{\rho_c v_c^2}{A_c} = 134 \pm 20\ \mathrm{J\,cm^{-3}}.$$

We fitted the results of Ref. 16, performed at $\lambda = 6328$ Å, in the same way and got $A_c = (1.06 \pm 0.15) \times 10^{-4}$, which gives a value in agreement $(\partial\mu/\partial c)^0_{\rho,T} = (103 \pm 20)\ \mathrm{J\,cm^{-3}}$.

We can therefore deduce the amplitude of the diverging susceptibility without any assumptions concerning light-scattering theories (Einstein, Yvon-Vuks, or Rocard).[18] It is interesting to check the value found for the universal amplitude ratio

$$R_\xi^+ R_c^{-1/3} = \xi_0 \left[B^2 \left(\frac{\partial \mu}{\partial c}\right)^0_{\rho,T} \Big/ k_B T_c\right]^{1/3},$$

where B is the amplitude of the coexistence curve defined as $(c^+ - c^-)/2 = B|t|^\beta +$ corrective terms, whose value is $B = 0.915 \pm 0.008$ in this mixture.[19] Our data lead to $R_\xi^+ R_c^{-1/3} = 0.72 \pm 0.07$ and those of Ref. 16 to $R_\xi^+ R_c^{-1/3} = 0.66 \pm 0.07$, in good agreement with the theoretical predictions[38,39] of 0.650 by the high-temperature-series method and 0.667 by renormalization-group calculations.

V. CONCLUSION

The study of the linewidth and the intensity of the Rayleigh-Brillouin spectrum versus $T - T_c$ in the weakly opalescent mixture of nitroethane and isooctane using a high-contrast spectrometer has

TABLE V. Fit of the Rayleigh-Brillouin Ratio to

$$\frac{I_R}{2I_B} = \left[A_c[1 + m\ (T - T_c)]\left(\frac{T - T_c}{T_c}\right)^{-\gamma} G(q\xi)\right] + (\gamma_0 - 1),$$

where $G(q\xi) = \sum_i b_i[1 + (\alpha_i q\xi)^2]^{-\mu_i}$ and (see text)

$b_1 = +1$, $\alpha_1 = 1.040\,056$, $\mu_1 = 1 - \eta/2 = 0.984\,25$,

$b_2 = +1$, $\alpha_2 = 1.058\,947$, $\mu_2 = \Omega = 1.554\,213$,

$b_3 = -1$, $\alpha_3 = 1.053\,932$, $\mu_3 = \Sigma = 1.627\,419$,

$m = 1.6 \times 10^{-3}\ \mathrm{K^{-1}}$, $q = 2.530 \times 10^5\ \mathrm{cm^{-1}}$, $\xi = \xi_0(1 - T/T_c)^{-\nu}$.

The parameters A_c, ξ_0, and γ_0 are considered as free parameters. The critical exponents γ and ν are universal and imposed to their expected value from a renormalization-group (RG) calculation (Ref. 38): $\gamma = 1.2402 \pm 0.0009$ and $\nu = 0.6300 \pm 0.0008$ [the values estimated by a high-temperature-series analysis are about the same (Ref. 39)].

Parameters	Results of the fit	Remarks
γ	1.2403 ± 0.0009	imposed within RG uncertainties
ν	0.6294 ± 0.0005	imposed within RG uncertainties
A_c	$(2.94 \pm 0.04) \times 10^{-4}$	free
ξ_0	2.42 ± 0.03 (Å)	free
$\gamma_0 - 1$	0.270 ± 0.001	free

Statistical quality coefficient = 0.841
Mean relative uncertainty = 3.02×10^{-2}

shown that neither the hypersonic velocity, the hypersound attenuation, nor the intensity of the Brillouin lines exhibit an anomalous behavior when approaching the critical point. The values which have been determined for these quantities are in the usual range for liquids. Moreover, the Rayleigh-Brillouin intensity ratio has allowed the ratio γ_0 of the specific heats to be accurately determined, with the correlation length amplitude ξ_0 and the susceptibility amplitude $[(\partial\mu/\partial c)^0_{p,T}]^{-1}$. It is worthwhile to note that this last parameter can be obtained without the usual local-field hypotheses (Einstein, Yvon-Vuks, or Rocard) which yield an ambiguous determination. Therefore, the universal amplitude ratio $R_\xi^+ R_c^{-1/3}$ has been obtained in agreement with the expected theoretical value.

ACKNOWLEDGMENTS

We gratefully thank B. Mozer and B. Le Neindre for their comments about this manuscript.

*On leave from Laboratoire des Interactions Moléculaires et des Hautes Pressions, C. N. R. S. Université Paris Nord, Avenue J. B. Clement, 93430 Villetaneuse, France.

[1]M. Fixman, J. Chem. Phys. 36, 1961 (1962).
[2]K. Kawasaki and M. Tanaka, Proc. Phys. Soc. London 90, 791 (1967).
[3]W. Botch and M. Fixman, J. Chem. Phys. 42, 199 (1965).
[4]J. M. Deutch and R. Zwanzig, J. Chem. Phys. 46, 1612 (1967).
[5]K. Kawasaki, Phys. Rev. A 1, 1750 (1970); 3, 1097 (1971).
[6]A. G. Chynoweth and W. G. Schneider, J. Chem. Phys. 19, 1566 (1951).
[7]I. M. Aref'ev, Zh. Eksp. Teor. Fiz. Pis'ma Red. 7, 361 (1968) [JETP Lett. 7, 285 (1968)].
[8]G. D'arrigo and D. Sette, J. Chem. Phys. 48, 691 (1968).
[9]I. M. Aref'ev and N. V. Shilin, Zh. Eksp. Teor. Fiz. Pis'ma Red. 10, 138 (1969) [JETP Lett. 10, 87 (1969)].
[10]I. M. Aref'ev and V. J. Birynkov, Zh. Eksp. Teor. Fiz. Pis'ma Red. 12, 352 (1970) [JETP Lett. 12, 240 (1970)].
[11]S. H. Chen and N. Polonsky, Phys. Rev. Lett. 20, 909 (1968).
[12]M. R. Kruer and R. W. Gammon, Bull. Am. Phys. Soc. 16, 84 (1971).
[13]C. S. Wang, Opt. Commun. 5, 56 (1972).
[14]M. I. Shakparonov, Yu. G. Shoroshev, S. S. Aliev, M. G. Khalinlin, and P. K. Khabibullaev, Zh. Fiz. Khim. 43, 2543 (1969) [Russ. J. Phys. Chem. 43, 1425 (1969)].
[15]A. Anisimov, I. M. Aref'ev, A. V. Voronel, V. P. Voronov, Yu. F. Kiyachenko, and I. L. Fabelinskii, Zh. Eksp. Teor. Fiz. 61, 1524 (1971) [Sov. Phys.—JETP 34, 813 (1972)]; I. M. Aref'ev and I. L. Fabelinskii, J. Phys. (Paris) 33, C1-131 (1972).
[16]I. M. Aref'ev, I. L. Fabelinskii, M. A. Anisimov, Yu. F. Kiyachenko, and V. P. Voronov, Opt. Commun. 9, 69 (1973).
[17]R. D. Mountain and J. M. Deutch, J. Chem. Phys. 50, 1103 (1969); P. Calmettes, thesis, Paris, 1969 (unpublished).
[18]For review, see D. Beysens, J. Chem. Phys. 64, 2579 (1976).
[19]D. Beysens, J. Chem. Phys. 71, 2557 (1979).
[20]D. Beysens and J. Wesfreid, J. Chem. Phys. 71, 119 (1979).
[21]D. Beysens and A. Bourgou, Phys. Rev. A 19, 2407 (1979).
[22]G. Zalczer and D. Beysens, J. Chem. Phys. 72, 348 (1980). Note that the value of η_0 is erroneous and must be changed from 2.82×10^{-4} P to 2.18×10^{-4} P.
[23]D. Beysens, Rev. Sci. Instrum. 50, 509 (1979).
[24]D. Beysens and G. Zalczer, Opt. Commun. 23, 142 (1977).
[25]D. Beysens and P. Calmettes, J. Chem. Phys. 66, 766 (1977).
[26]M. Tournarie, J. Phys. (Paris) 30, 47 (1969).
[27]Vogel, J. Chem. Soc. 1852 (1948); Wibaut, Rec. Trav. Chim. Pays-Bas Belg. 58, 374 (1939): quoted in Landolt-Bornstein, *Eigenschaften der Materie in Ihren Aggregatzuständen 8 Teil Optische Konstanten* (Springer, Berlin, 1962).
[28]P. Calmettes, Phys. Rev. Lett. 39, 1151 (1977).
[29]G. Carini, G. Maisano, P. Migliaro, and F. Wanderlingh, Phys. Rev. A 5, 1755 (1975).
[30]D. Beysens, S. H. Chen, J. P. Chabrat, L. Letamendia, J. Rouch, and C. Vaucamps, J. Phys. Lett. (Paris) 38, L-203 (1977).
[31]D. Beysens, M. Gbadamassi, and L. Boyer, Phys. Rev. Lett. 43, 1253 (1979).
[32]D. Beysens and G. Zalczer, Phys. Rev. A 18, 2280 (1978).
[33]D. Lister and D. E. Cooper, in Proceedings of the topical meeting in picosecond phenomena, edited by E. Ippen and C. V. Shank, North Falmouth, Mass., 1980 (unpublished); and D. E. Cooper, thesis, M.I.T., 1980 (unpublished).
[34]Note that the formula used in Ref. 19 to obtain the refractive index difference of the components from $(\partial n/\partial c)_{p,T}$ was approximate. Indeed, the derivative of the Lorentz-Lorenz LL formula for binary mixtures with nearly matched refractive indices leads to $(\partial n/\partial c)^{LL}_{p,T} = [(n_1 - n_2)]\,[(\rho/\rho_1) + (\rho/\rho_2)]$. Therefore, $(n_1 - n_2)$ can be estimated at 30 °C and 6328 Å: $(n_1 - n_2) = (1.36 \pm 0.04)\times10^{-3}$, which is somewhat different from the value 0.95×10^{-3} which was proposed.
[35]D. Beysens, A. Bourgou, and P. Calmettes (unpublished).
[36]J. C. Le Guillou and J. Zinn-Justin, Phys. Rev. B 21, 3976 (1980) and references therein.
[37]Phase Transitions: Status of the experimental and theoretical situations, edited by M. Levy, J. C. Le Guillou, and J. Zinn-Justin, Cargèse Summer Institute, 1980 (in press).
[38]A. Aharony and P. C. Hohenberg, Phys. Rev. B 13, 3081 (1976).
[39]C. Bervillier, Phys. Rev. B 14, 4964 (1976).